

HIGH ACCURACY MEASUREMENT OF THE HALL EFFECT IN MAGNETIC MATERIALS WITH AN A.C. LOCK'IN TECHNIQUE

J. B. SOUSA, J. M. MOREIRA

Centro de Física da Universidade do Porto
4000 Porto, Portugal

(Received 5 March 1982)

ABSTRACT— A very sensitive a. c. method is described for the measurement of the Hall effect in metals. It uses a high quality lock'in amplifier with the oscillator incorporated, an operational power supply, and a low noise step-up transformer to rise the signal level. Special precautions have been taken in the design of the experimental chamber and measuring circuit. Voltage resolutions down to 1 nV are currently achieved, enabling the Hall coefficient of most magnetic metals to be measured within 1 part in 10^3 .

A summary on the general transport equations and the correct definitions regarding the Hall effect in magnetic systems is presented. High accuracy data are given on the temperature dependence of the Hall resistivity (ρ_H) in a single crystal of Gadolinium, with the magnetic field in the basal plane. For the first time, we believe, experimental data have been obtained on the temperature derivative $d\rho_H/dT$. As shown here, this coefficient reveals clearly the critical behaviour associated with the ferro-paramagnetic transition point in Gadolinium. A preliminary analysis on the critical behaviour is given, with specific suggestions for further developments.

1 — INTRODUCTION

The investigation of the critical behaviour of transport properties in magnetic systems received considerable attention in the past, both in theory and experiment. The behaviour of the electrical resistivity is now satisfactorily understood [1], [2], followed by the case of the thermoelectric power [3]-[5] and, to a lesser extent, the thermal conductivity [3], [6]-[8]. The study of magnetic field effects on these transport coefficients near

a magnetic phase transition is also receiving increasing attention [9], [10].

The knowledge on higher-order transport phenomena, such as the thermo-magneto-galvanic effects, is rather scarce indeed [11]. The Hall effect stands however as a promising candidate for significant progress in the future [12].

For this reason we decided to implement a very sensitive and accurate method for the a.c. measurement of the Hall coefficient in metals, using a lock'in technique. The method described here also provides direct information on the transverse magnetoresistance coefficient. The voltage resolution is currently of the order of 10^{-9} V, enabling the Hall coefficient of most magnetic metals to be measured with a relative resolution better than 1:10³. The data reproducibility in different experimental runs is of the order of 1 part in 10³.

In section 2 we summarize the general transport equations, and give the correct definitions regarding the Hall effect and the magnetoresistance in magnetic systems, in order to set the precise experimental requirements. In section 3 the experimental method is described, with a brief reference to the errors and corresponding minimization procedures. In section 4 we report some representative data obtained with a characteristic ferromagnet (Gd single crystal; $T_c = 293$ K). Finally, a brief analysis of the main features present in the experimental curves for ferromagnets is given in section 5.

2 — THEORY

2.1 — *Transport coefficients in a magnetic field*

Usually, the electrical fields causing transport phenomena are sufficiently weak to be valid a linear approximation,

$$E_i = \rho_{ik} j_k \quad (1)$$

between the components E_i of the electrical field (\mathbf{E}) and the components j_k of the electrical current density (\mathbf{j}). The quantities ρ_{ik} define the electrical resistivity tensor for the material

under consideration. Isothermic conditions are assumed here and repetition of the k -index indicates a sum over all k -values (1, 2, 3).

In the presence of an internal magnetic induction (\mathbf{B}) the transport coefficients ρ_{ik} obey the Onsager relations [13]:

$$\rho_{ik}(\mathbf{B}) = \rho_{ki}(-\mathbf{B}) \quad (2)$$

One can separate ρ_{ik} into a symmetrical (s_{ik}) and an antisymmetrical part (a_{ik}):

$$\rho_{ik}(\mathbf{B}) = s_{ik}(\mathbf{B}) + a_{ik}(\mathbf{B}) \quad (3)$$

where

$$s_{ik}(\mathbf{B}) = s_{ki}(\mathbf{B}) = (1/2) [\rho_{ik}(\mathbf{B}) + \rho_{ki}(\mathbf{B})] \quad (4)$$

$$a_{ik}(\mathbf{B}) = -a_{ki}(\mathbf{B}) = (1/2) [\rho_{ik}(\mathbf{B}) - \rho_{ki}(\mathbf{B})] \quad (5)$$

The Onsager relations (2) imply the following symmetry for s_{ik} and a_{ik} :

$$s_{ik}(\mathbf{B}) = s_{ik}(-\mathbf{B}) \quad (6)$$

$$a_{ik}(\mathbf{B}) = -a_{ik}(-\mathbf{B}) \quad (7)$$

Substituting the decomposition (3) into (1) one gets:

$$E_i(\mathbf{B}) = s_{ik}(\mathbf{B}) j_k + a_{ik}(\mathbf{B}) j_k \quad (8)$$

Since the diagonal elements of a_{ik} are zero, this relation can be written in the equivalent form:

$$E_i(\mathbf{B}) = s_{ik}(\mathbf{B}) j_k + (\mathbf{j} \wedge \mathbf{A})_i \quad (9)$$

with

$$\mathbf{A} = (a_{23}, -a_{13}, a_{12}) \quad (10)$$

Or, in a more compact notation,

$$E_i = s_{ik} j_k + \varepsilon_{ikl} j_k A_l \quad (11)$$

where $\varepsilon_{ikl} = +1$ for $i, k, l = 1, 2, 3$ (or any even permutation), $\varepsilon_{ikl} = -1$ for odd permutations and zero otherwise.

Now the effects of the magnetic field are usually small, which justifies an expansion of the resistivity tensor components (s_{ik}, a_{ik}) in powers of B_i . Since a_{ik} is an odd function of the magnetic induction, \mathbf{A} is odd in \mathbf{B} . Therefore, the expansion of

the corresponding components involves only odd powers in B [13], [14]. Restricting the expansion to linear terms we have:

$$A_l = \alpha_{lm} B_m \quad (12)$$

The expansion of the even functions $s_{ik}(B)$ will involve only even powers, so that to second order we have:

$$s_{ik}(B) = s_{ik}(0) + \beta_{iklm} B_l B_m \quad (13)$$

The tensor β_{iklm} is symmetrical with respect to (i, k) and (l, m) . Substituting (12) and (13) into (11) we obtain, disregarding terms of the order $\mathcal{O}(B^3)$ or above:

$$E_i(B) = E_i(0) + \varepsilon_{ikl} j_k \alpha_{lm} B_m + \beta_{iklm} j_k B_l B_m \quad (14)$$

2.2 — *Hall effect*

As shown below, the Hall effect is related to the odd part of $E_i(\mathbf{B})$, whereas the magnetoresistance coefficients are related to the even part. Let us write:

$$E_i^{\text{odd}} = \varepsilon_{ikl} j_k \alpha_{lm} B_m \quad (15)$$

Performing formally the sum in l we can write:

$$E_i^{\text{odd}} = (\varepsilon_{ikl} \alpha_{lm}) j_k B_m = R_{ik}(m) j_k B_m \quad (16)$$

where $R_{ik}(m)$ is a generalized transport tensor corresponding to the B_m component of the magnetic induction,

$$R_{ik}(m) = \varepsilon_{ikl} \alpha_{lm} \quad (17)$$

As shown below it contains the usual Hall effect coefficient as one of its components. Since $\varepsilon_{ikl} = 0$ when two of the indices are equal, it follows that (for any i)

$$R_{ii}(m) = 0 \quad (18)$$

Also, since $\varepsilon_{ikl} = -\varepsilon_{kil}$, we have:

$$R_{ik}(m) = -R_{ki}(m) \quad (19)$$

Thus, the general form of the tensor $R_{ik}(m)$ involves only three distinct components

$$[R_{ik}(m)] = \begin{bmatrix} 0 & R_{xy}(m) & R_{xz}(m) \\ -R_{xy}(m) & 0 & R_{yz}(m) \\ -R_{xz}(m) & -R_{yz}(m) & 0 \end{bmatrix} \quad (20)$$

From eq. (17) it is clear that the crystal symmetry of the sample (contained implicitly in α_{im}) can lead to simplifications in the components $R_{ik}(m)$. For example, in isotropic media we have $R_{xz}(z) = R_{yz}(z) = 0$, so that:

$$[R_{ik}] = \begin{bmatrix} 0 & R & 0 \\ -R & 0 & 0 \\ 0 & 0 & 0 \end{bmatrix} \quad (21)$$

with $R = R_{xy}(z)$.

The odd components of the electrical field (E_i^{odd}) can be experimentally obtained from the components of the total field E_i measured for two opposite values of the magnetic field (H):

$$E_i^{\text{odd}} = 1/2 [E_i(H) - E_i(-H)] \quad (22)$$

For the geometry shown in Fig. 1 several distinct experiments may be considered:

(i) We can measure the odd component of the electric field in a direction normal to j and H , obtaining from eq. (16):

$$E_y^{\text{odd}} = E_y^{\text{Hall}} = R_{yx}(z) j_x B_z \quad (23)$$

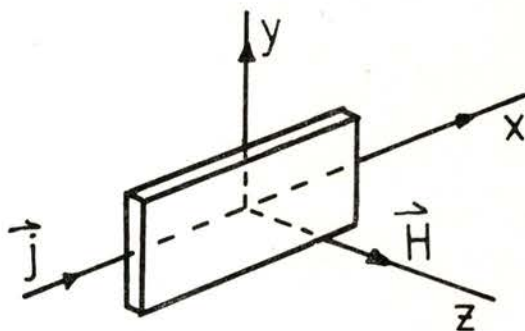


Fig. 1 — Geometry for the measurement of the Hall effect.

This corresponds to the usual Hall effect measurement, the component $R_{xy}(z)$ being precisely the Hall coefficient.

(ii) One can measure \mathbf{E}^{odd} along the z -direction (parallel to \mathbf{H}); eq. (16) then gives:

$$E_z^{\text{odd}} = R_{zx}(z) j_x B_z \quad (24)$$

which enables the coefficient $R_{zx}(z)$ to be experimentally determined.

(iii) Along the j -direction (x -axis), no odd electric field exists, since we have:

$$E_x^{\text{odd}} = R_{xx}(z) j_x B_z = 0 \quad (25)$$

If we want to know the coefficient $R_{zy}(z)$ we apply \mathbf{j} along the y -axis, measuring the odd component of the field along the z -axis:

$$E_z^{\text{odd}} = R_{zy}(z) j_y B_z \quad (26)$$

2.3 — Magnetoresistance

Let us consider the even part of the electric field:

$$E_i^{\text{even}} = E_i(0) + \beta_{iklm} j_k B_l B_m = [\rho_{ik}(0) + \beta_{iklm} B_l B_m] j_k \quad (27)$$

We can define a magnetoresistivity tensor

$$\rho_{ik}^m(\mathbf{B}) = \rho_{ik}(0) + \beta_{iklm} B_l B_m \quad (28)$$

which is an even function of B , so that:

$$E_i^{\text{even}} = \rho_{ik}^m(\mathbf{B}) j_k \quad (29)$$

Experimentally one obtains E_i^{even} from the total electric field components $E_i(\mathbf{B})$, measured for two opposite values of the magnetic field applied externally (\mathbf{H}_a):

$$E_i^{\text{even}} = (1/2) [E_i(\mathbf{H}_a) + E_i(-\mathbf{H}_a)] \quad (30)$$

Reassembling the results obtained in 2.2 and 2.3, we can write a general expression for the full electrical resistivity tensor (defined by eq. 1):

$$\rho_{ik}(\mathbf{B}) = \rho_{ik}(0) + R_{ik}(m)B_m + \beta_{iklm}B_lB_m \quad (31)$$

The quantities $R_{ik}(m), \beta_{iklm}, \dots$ are the so called galvanomagnetic coefficients.

2.4 — *Hall effect in ferromagnetic materials*

Assuming for simplicity an isotropic or cubic system with the geometry of Fig. 1, one gets for the Hall resistivity coefficient (eqs. 21, 31):

$$\rho_H = E_H/j = R_0 B \quad (32)$$

where $R_0 = R_{yx}(z)$, $B = B_z$, $E_H = E_y^{\text{odd}}$, $j = j_x$.

In a normal metal \mathbf{B} is simply given by $\mathbf{B} = \mu_0 \mathbf{H}_a$, where \mathbf{H}_a is the external magnetic field and μ_0 is the magnetic permeability of the medium (taken here equal to the vacuum permeability). However, for a magnetic material there are two additional contributions to \mathbf{B} , one from the internal magnetization \mathbf{M} and the other due to the demagnetisation field \mathbf{H}_d created by the discontinuity in \mathbf{M} at the surface of the medium. Then we have:

$$\mathbf{B} = \mu_0 \mathbf{H}_a + \mu_0 \mathbf{M} + \mu_0 \mathbf{H}_d \quad (33)$$

Assuming that the sample geometry can be approximately described by an equivalent ellipsoid, \mathbf{H}_d is related to the magnetization by the simple formula $\mathbf{H}_d = -D\mathbf{M}$, where D is the demagnetization factor of the equivalent ellipsoid. Then we obtain:

$$\mathbf{B} = \mu_0 \mathbf{H}_a + \mu_0 \mathbf{M} - \mu_0 D \mathbf{M} \quad (34)$$

This result should be inserted in eq. (32) to analyze the Hall effect. However, experiment shows that such a simple formula (eq. 32) does not work in magnetic materials.

The reason for this was the assumption that the transport coefficients were functions only of the magnetic induction \mathbf{B}

inside the medium. This induction \mathbf{B} is in fact responsible for the existence of a Lorentz force on the charge carriers which changes the corresponding trajectories, and then affects the transport coefficients.

However, in magnetic materials, besides the effects of \mathbf{B} on the electron trajectories between scattering centers, we must consider the possibility that the scattering events might themselves change the trajectories in a *preferential* way so as to give a net contribution for the Hall voltage. Of course, those scattering processes which give the same probability for electron deflections to the «right» or «left» of the initial \mathbf{k} -direction of the electron do not contribute to the Hall effect.

A careful analysis of the electron interaction with the ionic spins \mathbf{S}_i in a crystal lattice indeed shows that several processes exist which produce an asymmetric scattering [15], [16]. For example, the coupling of an ionic spin \mathbf{S}_i with the orbital momentum \mathbf{L} of an electron travelling in its vicinity does distinguish between right and left deflections, through the interaction term $\mathbf{S}_i \cdot \mathbf{L}/r^3$ (see Fig. 2). This term is independent of the electron

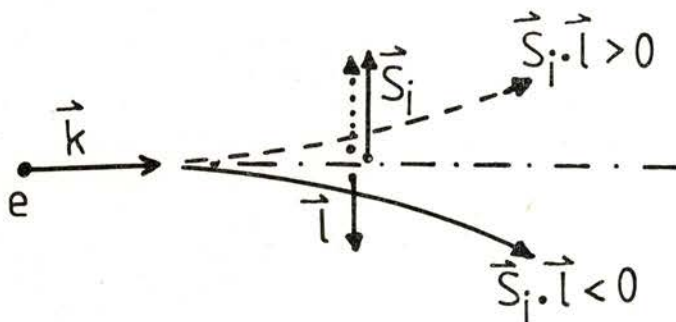


Fig. 2 — Asymmetric scattering resulting from the coupling of an ionic spin \mathbf{S}_i with the electron orbital momentum \mathbf{L}

spin, which means that spin up and spin down electrons are deflected in the same way. This is not sufficient to produce an Hall voltage. We need a *preferential* alignment of the spins \mathbf{S}_i in order to obtain a non-zero effect from scattering by different ions, i.e. there should exist a magnetization \mathbf{M} inside the sample. Thus, extra contributions to the Hall effect in magnetic materials are

expected below their magnetic ordering temperatures ($T < T_c$) [17]. Generally, these extra contributions first increase as T decreases (\mathbf{M} is enhanced) but as $T \rightarrow 0$ K full magnetic order takes place in the crystal and coherence effects on the electron wave function indeed suppress the scattering events. The Hall voltage thus vanishes as $T \rightarrow 0$ K.

Whereas for the Hall effect *both* the asymmetry of the scattering and the preferential magnetic alignment (\mathbf{M}) are simultaneously needed for its very existence, for most other transport coefficients important effects arise simply from the magnetic order in the system (\mathbf{M}). We can then write:

$$\rho_{ik} = \rho_{ik}(\mathbf{B}, \mathbf{M}) \quad (35)$$

and the Onsager relations can now be generalized:

$$\rho_{ik}(\mathbf{B}, \mathbf{M}) = \rho_{ki}(-\mathbf{B}, -\mathbf{M}) \quad (36)$$

Separating ρ_{ik} into a symmetrical and an antisymmetrical part, and developing the corresponding tensors in increasing powers of the components of \mathbf{B} and \mathbf{M} , one obtains for the odd part of the electric field components (in first order):

$$E_i^{\text{odd}} = R_{ik}^0(m) j_k B_m + R_{ik}^s(m) j_k \mu_0 M_m \quad (37)$$

where $R_{ik}^0(m)$ and $R_{ik}^s(m)$ are respectively the ordinary and the extraordinary Hall effect tensor components, when the external magnetic field is applied along the m -axis. For the geometry of Fig. 1 and in isotropic (or cubic) magnetic media, we have now the appropriate generalization of eq. (32):

$$\rho_H = R_0 B + R_s \mu_0 M \quad (38)$$

In the results (35)-(38) we are neglecting correlation effects between ionic spins; for example, ρ_{ik} might also depend on fluctuations of the form $\langle \mathbf{S}_i \cdot \mathbf{S}_j \rangle - \langle \mathbf{S}_i \rangle \cdot \langle \mathbf{S}_j \rangle$. These terms are certainly very important in the vicinity of a magnetic phase transition [18]. Unfortunately, the theory of the Hall effect is not yet fully developed to give an appropriate account of these effects.

3 — EXPERIMENTAL METHOD

3.1 — Principle of the method

A simple geometry for the Hall effect measurement is that of Fig. 1, with the Hall voltage (V_H , odd part) measured across the sample, in a direction normal both to \mathbf{j} and \mathbf{B} . From eq. (23) we readily obtain:

$$V_H = (R_H I B)/d \quad (39)$$

with $R_H = R_{yx}(z)$, $B = B_z$; I is the total electrical current (x -axis) and d is the thickness of the sample.

In normal metals, the fairly high values of the free-electron concentration leads to small values of the Hall coefficient ($R_H \lesssim 10^{-10} \Omega \cdot \text{m} \cdot \text{T}^{-1}$). In order to increase V_H the samples then need to be as thin as possible, and usually we have $d \lesssim 1$ mm for bulk samples. Even under these favourable conditions, the use of $B \sim 1$ T and $I \sim 1$ A produces Hall voltages of only $0.1 \mu\text{V}$. In order to achieve 1% resolution in the corresponding measurement, we must then have at least 1 nV voltage sensitivity.

In magnetic materials the Hall coefficient can be considerably higher in the cooperative phase ($R_H \sim 10^{-9} \Omega \cdot \text{m} \cdot \text{T}^{-1}$) and then a resolution of 1 part in 10^3 becomes possible within 1 nV resolution in the voltage measurements. Of course, the voltage stability must be maintained at this level when reversing the magnetic induction from $+\mathbf{B}$ to $-\mathbf{B}$.

In order to achieve such high degree of voltage resolution and stability one is forced, almost invariably, to rule out d.c. methods. Even if we had solved all the noise problems and maintained the required stability of the measuring equipment, unavoidable parasitic d.c. thermal emf's would appear in the sample or along the leads in the cryostat, including those produced by the inversion of \mathbf{B} [13]. For these reasons we adopted an a.c. method, and in order to minimize noise problems we used a lock'in technique.

Fig. 3 shows a schematic diagram of the experimental set up. A high stability oscillator, with frequency adjustable from 0.5 Hz to 100 KHz, provides both the reference signal for the lock'in

amplifier (Ortec 9501D) and the input signal for the operational power supply providing the current I for the sample (Kepko BOP50-2M; 0-3A). The sample had the shape of a thin slab with three Pt (or Cu) contacts spotwelded in the opposite edges of the middle portion (two on one side, about a fraction of a mm apart). These electrical contacts enabled the transverse voltage to be measured and also the «zero» adjustment at $B = 0$, through a 10 Ω , 20 turns potentiometer shown in Fig. 3.

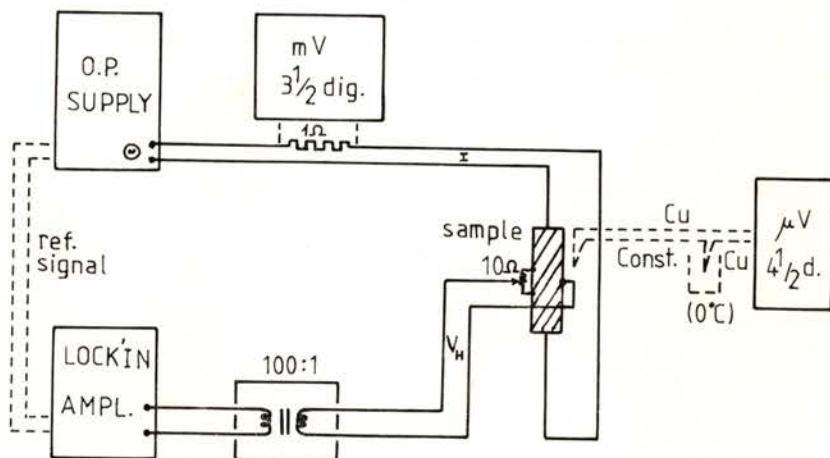


Fig. 3 — Block diagram of the experimental set up for the Hall effect measurement.

The transverse (Hall) voltage was amplified just at the top of the cryostat by a low noise, high quality step up signal transformer (1:100; Ortec 9433). This ensured a proper level of the signal outside the cryostat ($\geq 1 \mu$ V), just when the measuring circuit is more exposed to noise and pick-up signals from external sources. The output of the transformer was fed into the lock'in phase sensitive detector, where it was amplified again. This detector provided a digital display (3 1/2 digits) up to a resolution of 1 nV.

The current I through the sample was measured to within 1 part in 10^3 on a digital voltmeter (Philips PM 2421), using the voltage drop produced in a stable 1 Ω resistor.

3.2 — *Auxiliary equipment and experimental details*

In order to measure the Hall effect over a wide range of temperature (77-340 K) a standard metallic cryostat was used (Fig. 4), with a tail in the lower part to fit the 6 cm pole gap of a conventional electromagnet (Newport; 0-15 KOe). A high stability d.c. current power supply (± 1 in 10^5) provided an adjustable current up to 30 A for the electromagnet. A sweep unit enabled a wide range of energization rates to be used for the electromagnet. A servo-unit enabled the remote control of the electromagnet (on-off, reverse, and sweep modes).

The magnetic field was measured with a calibrated transverse Hall probe (Phillips RHY17; see Fig. 5a), placed within the pole gap of the electromagnet, with a sensitivity of the order of $10^3 \mu\text{V}/\text{KG}$ per mA. Using a Hall-probe current of 5 mA and having voltage resolutions of $10 \mu\text{V}$ (read in a 3 1/2 digit voltmeter), a field resolution of 2 G was possible.

The temperature was measured with a copper-constantan thermocouple, with one of its junctions in an ice-water bath and the other in good thermal contact with the sample. The sample was mounted on a thick copper block (glued with varnish) and surrounded by a metallic shield to homogenize the temperature in the experimental chamber. The temperature could be raised from 77 K to room temperature at a fairly small rate (as low as a few mK per min) by the combined action of Joule heating in a small heater in the experimental chamber and the adjustment of the vacuum conditions in the dewar. The emf of the thermocouple was measured directly on a 5 1/2 digit voltmeter ($0.1 \mu\text{V}$ resolution), so that temperature resolutions of the order of a few mK were easily achieved.

The electrical contacts were made with thin wires of Pt or Cu ($\varnothing = 0.05\text{-}0.1$ mm) directly spotwelded into the sample using a capacitive discharge unit locally constructed [19]. In an earlier stage we tried pressure contacts, made of elastic copper-berilium wires, but the differences in thermal expansion coefficients of the different materials produced minute relative displacements between sample and contacts as the temperature changed in the

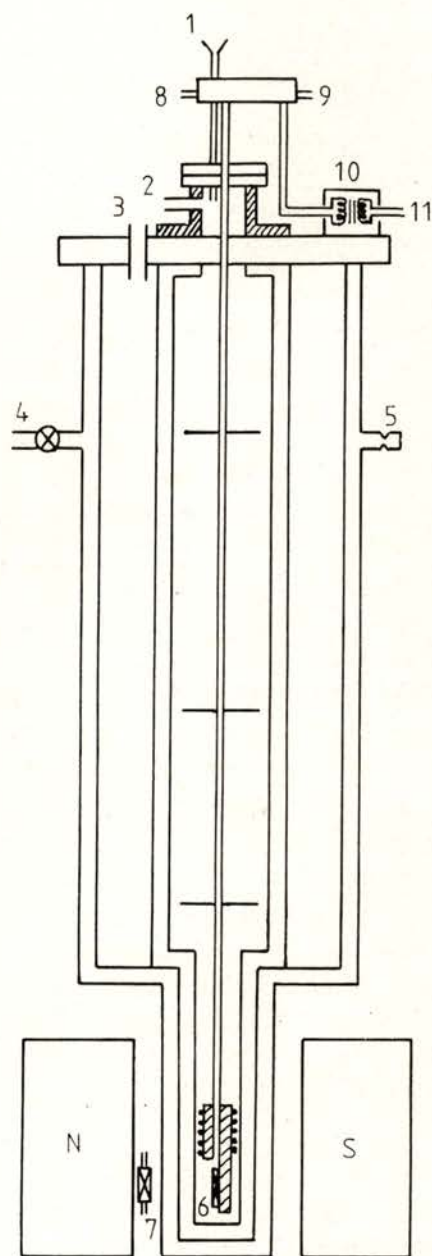


Fig. 4—Cryostat and auxiliary equipment: 1—filling tube (N_2 or He); 2—pumping line (bath); 3—nitrogen tube; 4—vacuum (to pump); 5—safety valve; 6—sample; 7—Hall probe; 8—current to the sample; 9—thermocouple voltage; 10—step up transformer (1:100); 11—Hall voltage ($\times 100$).

cryostat. This produced a significant and erratic increase in the scatter of the experimental points, and also in the «zero» drift. Besides the measurement of the Hall coefficient as a function of temperature under a constant applied magnetic field (H_a) we could also measure the field dependence of the Hall voltage at constant temperature. For this we used an automatic data acquisition system locally constructed which could measure simulta-

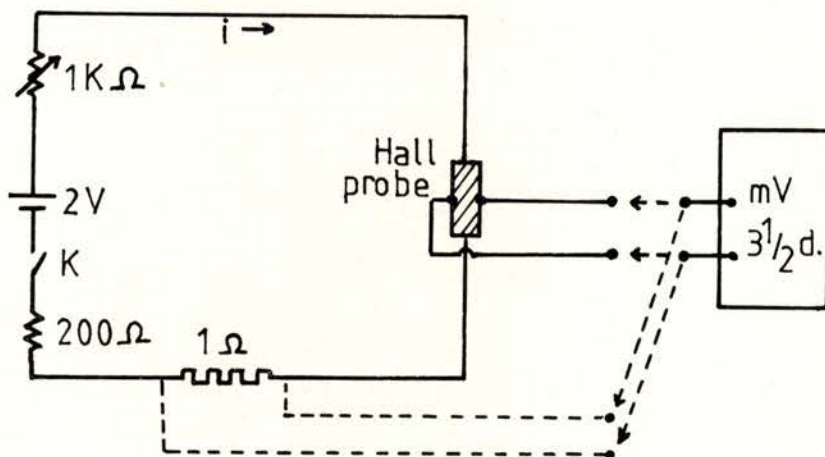


Fig. 5-a — Circuit for the measurement of the applied magnetic field.

neously, and every 3 s (adjustable for longer periods), the Hall voltage V_H and the field H_a , performing automatically the derivative dV_H/dH_a over an adjustable period of time, typically of the order of 1 min. A slow sweep of the field H_a (e.g. over 10 min) enabled a fairly detailed knowledge of the field dependence $V_H = V_H(H_a)$ at constant temperature.

The experimental resolution of the Hall data as a function of temperature was sufficiently good to enable an accurate knowledge of the temperature derivative dV_H/dT at any particular temperature. This was done with the so called «sliding rule» method, using always a set of 3 (or 5) experimental points (V_H, T) to compute the corresponding derivative within such interval. This process was repeated along the whole set of experimental data points in order to obtain the complete curve dV_H/dT as a function of temperature.

3.3 — Experimental errors

3.3.1 — Spurious voltages in the measuring circuit

a) In order to minimize the Johnson noise, the electrical resistance of the measuring circuit was kept as low as possible, the major resistive component being the potentiometer for the zero adjustment. As a compromise between its resistance and resolution, we used a 20 turns, 10 Ohm helipot. This gives a thermal noise of about $0.5\text{nV}/\sqrt{\text{Hz}}$ at room temperature, which is negligible for our purposes.

In order to analyze other errors, it is convenient to use the equivalent circuit of Fig. 5b, introducing the current I and the

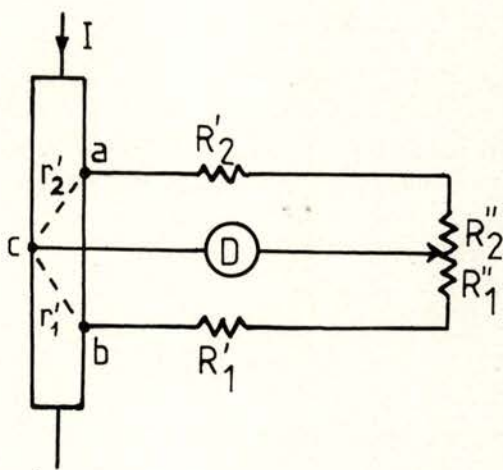


Fig. 5-b — Equivalent circuit of sample + leads + potentiometer resistances, for the analysis of errors; $R_1 = R'_1 + R''_1$, $R_2 = R'_2 + R''_2$.

resistances of each lead + corresponding branch in the potentiometer (R_1 , R_2 ; see Fig. 5b), and the sample resistance on both sides of the central electrical contact (r_1 , r_2). In principle the parameters R_1 , R_2 , r_1 , r_2 and I should be constant, but this never happens exactly in practice and so a spurious voltage (δv) appears

in the measuring circuit. For small changes in the above parameters one can show that:

$$\delta v = v_H \frac{\delta I}{I} + V \delta \left(\frac{R_1}{R_1 + R_2} \right) - V \delta \left(\frac{r_1}{r_1 + r_2} \right) \quad (40)$$

where $V = (r_1 + r_2) I$. In our case, $I = 0.5$ A, $V \sim 10^3 \mu\text{V}$, $v_H \sim \mu\text{V}$, $R_1 + R_2 \sim 10 \Omega$, $r_1 + r_2 \sim \text{m}\Omega$.

b) The drift voltage associated with the current [$v_H (\delta I/I)$] is usually negligible. For example, with a (poor) current stability of $1:10^3$ such voltage is only of 1 nV, since v_H is itself fairly small ($\sim \mu\text{V}$).

The errors due to the relative changes in the resistances produced by changes of temperature demand far greater care, since they appear multiplied by the longitudinal voltage in the sample, $V \sim 10^3 \times v_H$.

c) Let us consider first the term which involves the changes of the leads and potentiometer resistances with temperature. Since the potentiometer is at room temperature and outside the cryostat, it is not difficult to have proper thermal insulation so as to eliminate virtually the changes in its resistance during the measurements. The above expression then leads to:

$$V \delta \left(\frac{R_1}{R_1 + R_2} \right) \simeq \frac{R_1 R_2}{(R_1 + R_2)^2} \left[\frac{\delta R'_1}{R_1} - \frac{\delta R'_2}{R_2} \right] V \quad (41)$$

where $\delta R'_1$, $\delta R'_2$ are the changes in the leads resistances due to changes in temperature. In practice we can easily set the conditions to have the balance of the potentiometer close to its middle point ($R_1 \simeq R_2$), so that:

$$V \delta \left(\frac{R_1}{R_1 + R_2} \right) \simeq \frac{1}{4 R_1} (\delta R'_1 - \delta R'_2) V \quad (42)$$

One way to minimize this error is to use leads closely matched in diameter and length, and following the same path along the cryostat in order to ensure the same thermal effects ($\delta R'_1 \simeq \delta R'_2$).

d) With regard to the temperature effects in the sample, the corresponding error can be written as:

$$V \delta \left(\frac{r_1}{r_1 + r_2} \right) \approx V \left[\frac{1}{\rho} \frac{d\rho}{dT} - \alpha \right] \delta T \quad (43)$$

where ρ is the sample resistivity, α the linear expansion coefficient, and δT is the difference of temperature between the voltage contacts (a, b in Fig. 5b). With a careful mounting of the sample (in good thermal contact with a copper basis) one can easily ensure that $\delta T \lesssim 10^{-2}$ K. Since $\alpha \sim 10^{-5}$ K $^{-1}$ and $(1/\rho)(d\rho/dT) \sim 10^{-3}$ K $^{-1}$, we get a non-negligible voltage of the order of 10 nV. For a given difference of temperature δT in the sample this originates a systematic error in the measurement (see 3.3.2).

3.3.2 — Elimination of systematic errors

a) In order to eliminate spurious voltages which are even functions of the magnetic field we invert \mathbf{H} and take half of the difference between the corresponding voltage readings (see eq. 30). This procedure also eliminates the thermal gradient effects which are independent of \mathbf{H} , when the operation $(\mathbf{H}) \rightarrow (-\mathbf{H})$ is sufficiently quick, so as to keep the thermal gradients practically the same during the switching operation.

b) The use of an alternating technique completely eliminates the effect of all parasitic d.c. voltages in the measuring circuit, and of the effects which are even functions of the electrical current I . This includes all the thermal gradient effects independent of the sense of I , which would produce spurious voltages, e.g. through the Nernst effect: a longitudinal temperature gradient originates a transverse voltage under \mathbf{H} [11].

c) There are, however, thermal gradients associated with the *sense* of the electrical current (e.g. Peltier heating or cooling: odd parity in I) and so not eliminated through the current reversal procedure. However, using an a.c. current of sufficient frequency (e.g. above ~ 20 Hz) one can severely reduce the building up of thermal gradients in either sense during the correspondingly small period used. This is particularly useful to reduce the Ettinghausen

effect, which has exactly the same parity as the Hall effect with respect to I and H (a longitudinal current I produces a transverse gradient under H). Other considerations on the Hall effect measurement can be found in the literature [13], [20]-[22].

3.3.3 An experimental check on stability and reproducibility.

After completion of the several stages of implementation of our experimental method, a thorough check was made on the stability and reproducibility of the equipment under realistic working conditions. For such purpose we mounted a Gd single crystal in the cryostat under an applied magnetic field of $7.7 \times 10^5 \text{ A.m}^{-1}$ (9.7 KOe), and measured the corresponding Hall voltage from 77 up to 273 K in two different runs, performed in different days. The table below shows that the Hall voltages measured in each run (V_1 , V_2) could be reproduced to within a few nV. Since each run takes an average of 24 hrs, we can also claim a comparable degree of stability of the measuring equipment over such a period of time.

T (K)	V_1 (μV)	V_2 (μV)
77.231	1.959	1.957
92.594	2.530	2.534
102.779	2.854	2.855
121.685	3.446	3.443
130.536	3.700	3.703
143.192	4.135	4.130
155.210	4.602	4.597
166.679	5.113	5.108
177.673	5.876	5.867
188.248	6.810	6.812
198.452	7.989	7.984
211.544	9.748	9.740
224.118	11.749	11.741
236.235	13.985	13.972
250.812	16.647	16.621
262.067	18.370	18.347
272.999	19.016	19.012

4 — EXPERIMENTAL RESULTS

Fig. 6 shows the temperature dependence of the Hall resistivity ρ_H , from 77 K up to 330 K, measured in a single crystal of gadolinium with dimensions of 12.5 mm \times 2.20 mm \times 0.455 mm.

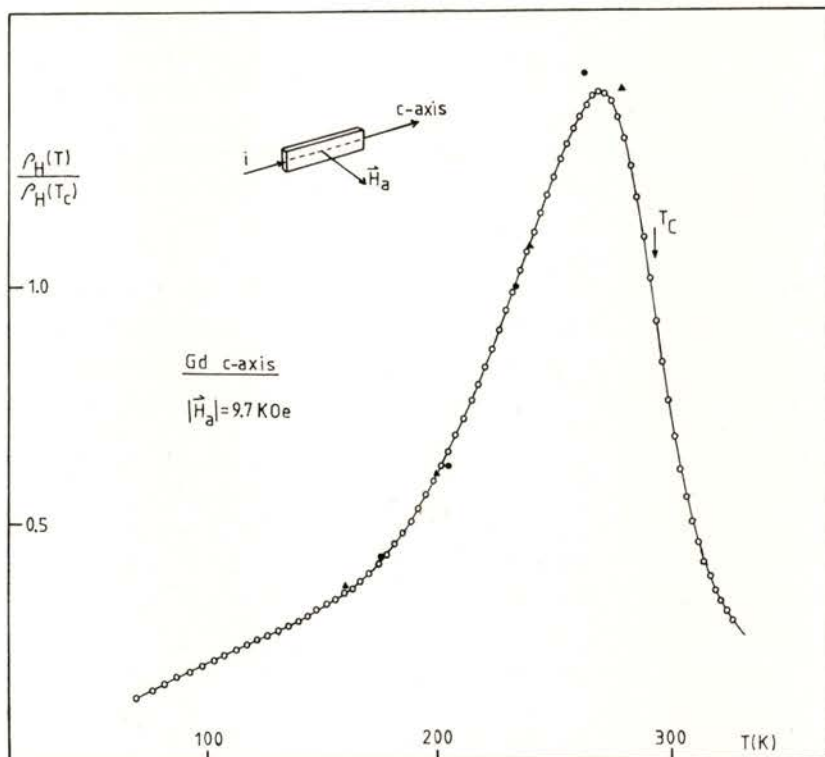


Fig. 6 — Temperature dependence of the Hall electrical resistivity (ρ_H) in a single crystal of Gd, normalized by a factor $\rho_H(T_c)$, with $T_c = 293$ K. (•) data from ref. [18] (▲) data from ref. [30] (see text).

For convenience, we present our data normalized by a factor $\rho_H(T_c)$, with $T_c = 293$ K as shown below. The electrical current flows along the c -axis, which is the major dimension of the sample. The external magnetic field (H_a) was always perpendicular to the flat face of the crystal, thus having a basal

direction. For the data of Fig. 6 we used $H_a = 7.7 \times 10^5 \text{ A.m}^{-1}$ (9.7 KOe).

The experimental curve exhibits all the qualitative features predicted by theory: (i) at low temperatures the Hall effect decreases noticeably with T , due to the reduction in the electron scattering as the sample orders magnetically; (ii) at higher temperatures ($T \geq 150 \text{ K}$), there is a noticeable increase in the Hall resistivity, associated with the production of magnetic disorder in the system; (iii) with the approach of T_c , and in spite of the increasing magnetic disorder, ρ_H decreases sharply due to the vanishing of the spontaneous magnetization in the sample; (iv) however, the decrease of ρ_H still continues in the paramagnetic phase, due to the persistence of an induced magnetization under the applied field; it naturally decreases with the increase of T , as the magnetic susceptibility falls off in the paramagnetic phase.

A better insight into the reduction of the Hall effect near the Curie point can be obtained from the temperature derivative curve $d\rho_H/dT$ as a function of T . This quantity was calculated by numerical differentiation of $\rho_H(T)$, using groups of five consecutive experimental points, slid along the $\rho_H(T)$ curve. The results are shown in Fig. 7, normalized by the quantity $\rho_H(T_c)$.

There is a deep minimum in the derivative $d\rho_H/dT$ at the critical region, with the lowest point at 293 K approximately. This temperature has been identified with the Curie point of our Gd sample. It is in fact consistent with corresponding data available in the literature [23], [24]. The $[1/\rho_H(T_c)](d\rho_H/dT)$ curve exhibits an approximately constant value for temperatures below $\sim 150 \text{ K}$, which means an approximately linear dependence of ρ_H with T at these temperatures. A change in regime occurs for $T \geq 150 \text{ K}$, as evidenced by the pronounced rise in $[1/\rho_H(T_c)](d\rho_H/dT)$ towards a broad maximum around 230-240 K. It should be recognized that Gd has a spin-reorientation transition in zero field at temperatures close to these values [25], [26]. The spontaneous magnetization in Gd then turns rapidly from a cone easy axis towards the c -direction. We indeed found that this transition produces a striking anomaly in the even-part of the transverse voltage, an observation which appears not to be referred previously in the literature. These results will be the object of a forthcoming publication.

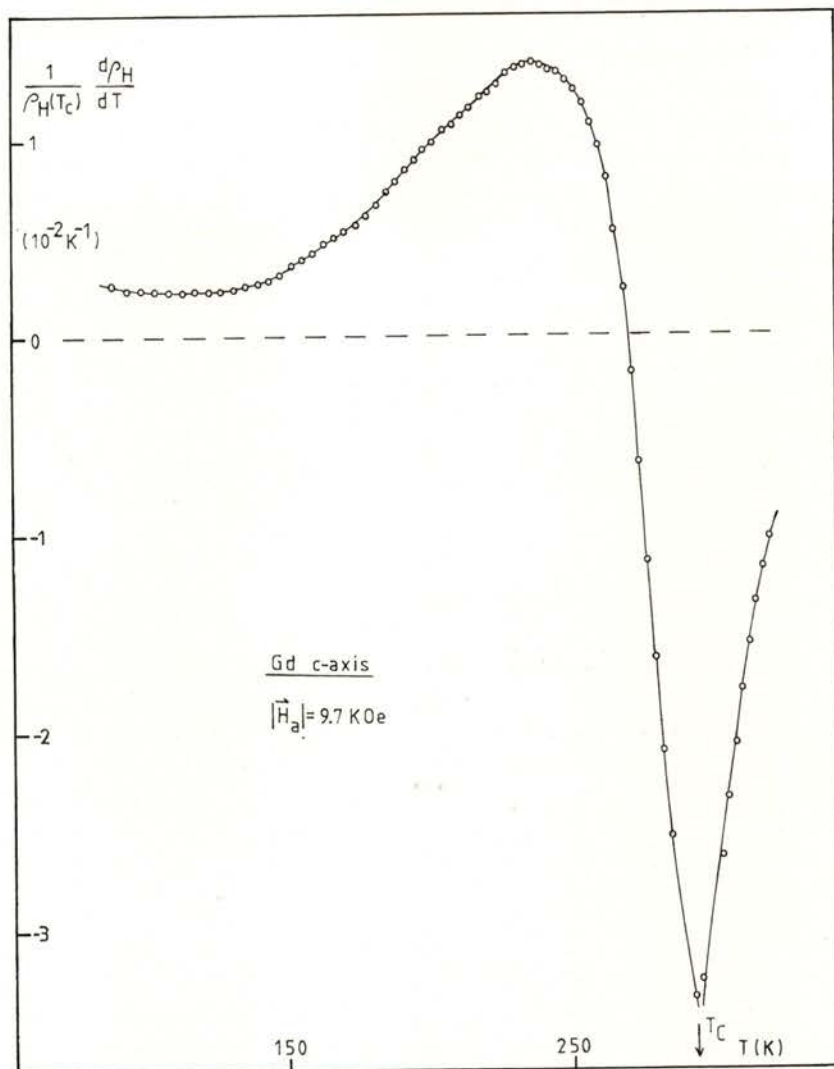


Fig. 7— Temperature derivative of the normalized Hall electrical resistivity as a function of temperature.

5 — ANALYSIS AND DISCUSSION

5.1 — Ferromagnetic phase

a) $T \lesssim 270 \text{ K}$:

Due to the high demagnetization factor of the sample under the conditions of measurement ($D \simeq 1$), and the use of a moderate

value for H_a ($\lesssim 10$ KOe; in Gd the saturation field at low temperatures exceeds 26 KOe [27]), magnetic field penetration is not expected at these temperatures (see 5.1.b). In good quality samples we then expect that the magnetic domain structure inside the sample adjusts itself at each temperature so as to keep a vanishing internal magnetic field. Since $H_i = H_a - D M$, this produces a temperature independent bulk magnetization in the sample:

$$M = (1/D) H_a \simeq H_a \quad (44)$$

This magnetization represents a coarse average over many magnetic domains, and should not be confused with the spontaneous magnetization inside each domain, $M_s(T)$; we have in fact $M \leq M_s$. The average magnetic induction in the sample is then:

$$B = \mu_0 (H_i + M) \simeq \mu_0 M \simeq \mu_0 H_a \quad (45)$$

and we obtain for the Hall resistivity:

$$\rho_H = R_0 B + R_s \mu_0 M \simeq (R_0 + R_s) \mu_0 H_a \quad (46)$$

At constant H_a , the temperature dependence of ρ_H essentially reflects the corresponding dependence of $(R_0 + R_s)$. Since in Gd the coefficient R_0 is approximately two orders of magnitude smaller than R_s [18], [28], [29], our Hall resistivity at T sufficiently below T_c ($H_i \simeq 0$) essentially gives the behaviour of the extraordinary Hall coefficient:

$$\rho_H(T) \simeq \mu_0 H_a R_s(T) \quad (47)$$

In order to check this, a direct comparison was made between the normalized $\rho_H(T)$ data of Fig. 6 and $R_s(T)$ values published in the literature for Gd single crystals, with H_a along a basal direction [18], [30]. As shown by the full circles and the triangular symbols in Fig. 6, fairly good agreement is indeed obtained, with a normalization constant chosen to match all the data at $T=237$ K.

b) $270 \lesssim T < T_c$:

The condition $H_i \simeq 0$ used above is expected to break down when the spontaneous magnetization decreases sufficiently (as $T \rightarrow T_c$) so as to be no longer able to prevent field penetration.

As shown below, this originates the appearance of a maximum in the $\rho_H(T)$ curve of Fig. 6 ($H_a = 9.7$ KOe). Such maximum is not a characteristic feature of the extraordinary Hall coefficient $R_s(T)$ (monotonic increasing function of T), but a consequence of the fact that $\rho_H(T)$ contains the product $R_s(T) M(T)$.

Whereas no field penetration occurs at low temperatures ($H_i \approx 0$; $M = \text{constant} = H_a/D$), the situation changes as we approach a temperature T^* for which the spontaneous magnetization $M_s(T)$ gets smaller than H_a/D . We then expect $M \approx M_s(T)$ and a single domain situation. Using $D = 1$, $H_a = 9.7$ KOe, and calculating $M_s(T)$ within a mean field approximation (see 5.2) we arrive at $T^* = 270.1$ K, which is indeed remarkably close to the temperature at which ρ_H is maximum ($T = 270 \pm 1$ K).

As the spontaneous magnetization is a decreasing function of T , the condition:

$$D M_s(T^*) = H_a \quad (48)$$

predicts the gradual shift of the maximum in ρ_H to the right, as the field H_a decreases. This is clearly shown in Fig. 8, for $H_a = 7.7 \times 10^5$, 3.87×10^5 and 2.0×10^5 A.m⁻¹ (9.7, 4.87 and 2.52 KOe, respectively).

c) Theoretical considerations.

The general features of ρ_H in the ferromagnetic phase of Gd are: (i) a gradual increase of ρ_H from low temperatures upwards ($\sim T^2$ dependence [31]) and (ii) a well defined maximum at high temperatures, just preceding the rapid decrease of ρ_H as T approaches the Curie point. Since $R_0 \ll R_s$ in gadolinium [29], we have $\rho_H(T) \approx R_s(T) M(T)$.

The observed temperature dependence of ρ_H in gadolinium has been successfully described by the theory of Maranzana [32], based on the asymmetric scattering of electrons by thermal spin disorder through the coupling between the orbital angular momentum of the conduction electrons and the localized magnetic moments. Maranzana uses a mean field approximation and assumes a single domain in the sample ($M(T) = M_s(T)$), giving an explicit expression for the extraordinary Hall resistivity:

$$R_s(T) M_s(T) = A \langle (S_z - \langle S_z \rangle)^3 \rangle \quad (49)$$

A is a constant independent of the temperature, S_z is the z-component of an ionic spin, and $\langle \dots \rangle$ represents a thermal average

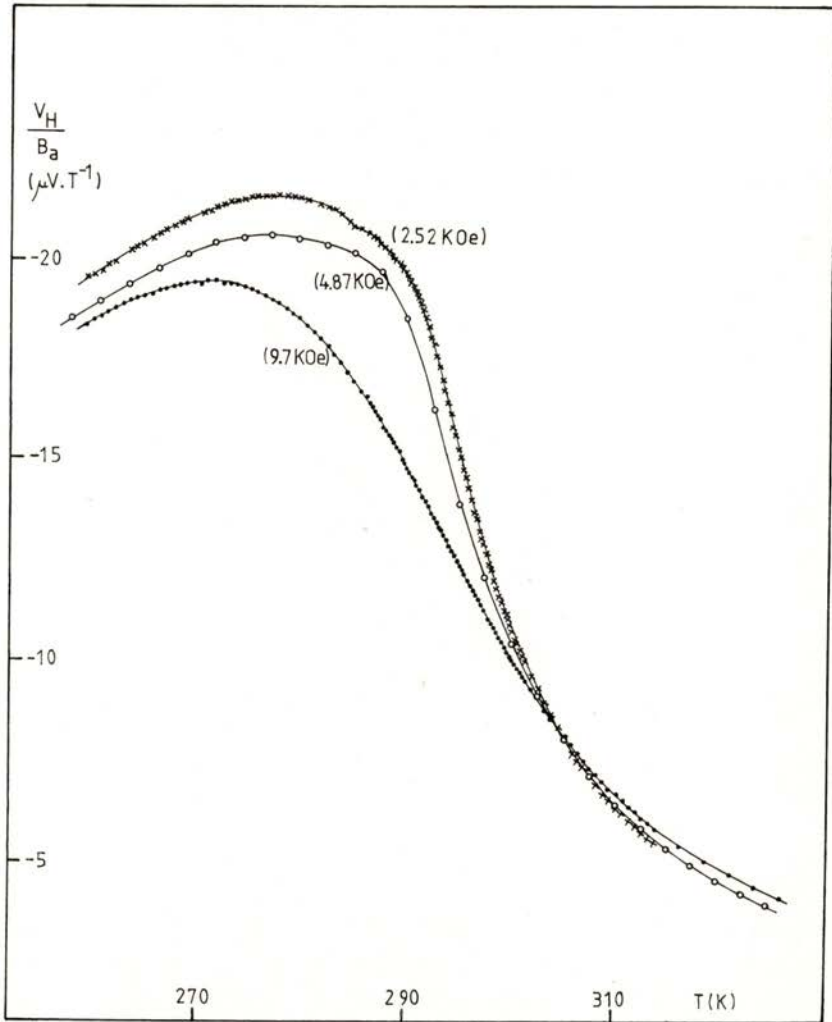


Fig. 8 — Temperature dependence of the Hall voltage (v_H), normalized by $B_a = \mu_0 H_a$, at several values of B_a : 0.97, 0.487 and 0.252 T.

over all possible values of the z-component of a spin at a single lattice. As a mean field model, Maranzana's theory cannot be valid

very near T_c , where fluctuations dominate. If we work out the $\langle \dots \rangle$ factor in expression (49) we can show that:

$$\begin{aligned} \langle (S_z - \langle S_z \rangle)^3 \rangle &= [\langle S_z^3 \rangle - \langle S_z \rangle^3] - 3\langle S_z \rangle [\langle S_z^2 \rangle - \langle S_z \rangle^2] \\ &= [-2\langle S_z \rangle + \coth(\alpha/2)] [\langle S_z^2 \rangle - \langle S_z \rangle^2] + 1/2 \langle S_z \rangle \operatorname{sech}^2(\alpha/2) \end{aligned} \quad (50)$$

where $\alpha = 3S/(S+1) \langle S_z \rangle (T_c/T)$. For temperatures reasonably below T_c and for systems with $S \gg 1/2$ ($S = 7/2$ in Gd), the second and third terms on the right hand side of (50) are considerably smaller than the first, and we can write approximately [33]:

$$\rho_H \sim \langle (S_z - \langle S_z \rangle)^3 \rangle \approx -2 \langle S_z \rangle [\langle S_z^2 \rangle - \langle S_z \rangle^2] \quad (51)$$

This expression has a very simple physical meaning: the extraordinary Hall effect requires the existence of electron scattering [$\langle S_z^2 \rangle - \langle S_z \rangle^2$] and the existence of a finite magnetization in the sample, $\langle S_z \rangle$. One can now understand the general trend of $\rho_H(T)$ in gadolinium, as a result of two factors: a monotonically increasing function of temperature, [$\langle S_z^2 \rangle - \langle S_z \rangle^2$] (responsible for the initial rise of ρ_H with T), multiplied by a monotonically decreasing function of T , $\langle S_z \rangle$ (responsible for the sharp decrease of ρ_H near T_c). A maximum in ρ_H thus occurs due to the competing effect of both factors. It occurs rather close to T_c because at low temperatures $\langle S_z \rangle$ has a rather weak temperature dependence, which cannot prevent the increase in ρ_H caused by the other factor.

Unfortunately, Maranzana's theory is unable to justify the large magnitude of R_s in Gd, although it appears quite satisfactory to explain the temperature dependence of $R_s(T)$ [28], [34]. An alternative theory, based on the side jump mechanism for the collisions between electrons and the (thermally disordered) localized spins, has been worked out by Fert [35]. This theory can also explain rather well the temperature dependence of ρ_H in Gd and, for quantitative purposes, it requires more reasonable values for some adjustable parameters than in the case of Maranzana's theory. We feel, however, that more experimental and theoretical work is needed to clarify definitely this interesting question related to the scattering mechanism ultimately responsible for the magnitude of ρ_H in Gd [39].

5.2 — Paramagnetic phase

a) Our experimental data show a progressive decrease of $\rho_H(T)$ in the paramagnetic phase, essentially reflecting the decrease of the induced magnetization $M(T)$ inside the sample; of course, no spontaneous magnetization $M_s(T)$ exists above T_c . From expression (38) we can write:

$$\begin{aligned} \rho_H &= R_0 B + R_s \mu_0 M = R_0 \mu_0 (H_i + M) + R_s \mu_0 M \\ &= R_0 \mu_0 H_a + \mu_0 [R_s + (1 - D) R_0] M \end{aligned} \quad (52)$$

Since $D = 1$ in our case, $\rho_H(T)$ in the paramagnetic phase can be approximated by the simpler expression:

$$\rho_H(T) = \mu_0 R_0 H_a + \mu_0 R_s M(T) \quad (53)$$

Excluding the immediate vicinity of T_c , the theory predicts that R_s becomes constant in the paramagnetic phase [28], [33]. Since $R_0 \ll R_s$, this means that the temperature dependence of the measured Hall resistivity in the paramagnetic phase should essentially reproduce the T -dependence of the induced magnetization $M(T)$. One can calculate this quantity within a mean field approximation, using the standard expression [36]:

$$\begin{aligned} M(T)/M(0) &= B_s [\mu_0 g \mu_B S H_i / (K T_c)] \cdot (T_c/T) + \\ &+ 3 S / (S + 1) \cdot M(T)/M(0) (T_c/T) \end{aligned} \quad (54)$$

where B_s is the Brillouin function,

$$B_s(x) = (2S + 1)/S \cdot \coth x - (1/2S) \coth x/2S \quad (55)$$

H_i is the internal magnetic field, $H_i = H_a - DM$, g is the Landé factor and μ_B is the Bohr magneton. Introducing $M(T)$ calculated in this way into expression (53), we can separate R_0 and R_s from a fit to the experimental data on $\rho_H(T)$.

The simpler approach generally adopted is to go into the asymptotic form of $M(T)$ at temperatures sufficiently above T_c , where a simple Curie-Weiss behaviour is expected:

$$M(T) = C / (T - \Theta) \cdot H_i = \chi(T) \cdot H_i \quad (56)$$

with $C = \text{constant}$, $\Theta = \text{paramagnetic Curie temperature}$. Experiment gives $\Theta = 317 \text{ K}$ and $C = 0.05 \text{ K}$ for Gd [27]. Introducing $H_i = H_a - \text{DM}$ in this expression we obtain:

$$M(T) = \chi / (1 + \chi D) H_a \approx \chi / (1 + \chi) H_a = C / (T - T_c^*) \quad (57)$$

where $T_c^* = \Theta - C$.

However, experiment shows that the Curie-Weiss behaviour in Gd is only valid for $T \geq 400 \text{ K}$, which is well outside the temperature range covered by our data. We must therefore use the full mean field expression (54) to obtain $M(T)$ values in the paramagnetic range order to analyze our data.

b) For Gd we used $S = 7/2$, $M(0) = 2.10 \times 10^6 \text{ A.m}^{-1}$ (26.4 KOe) [27], $T_c = 293 \text{ K}$, and $D = 1$ under our experimental conditions. The field H_a was allowed to take the three distinct values used in our experiments: $H_a = 2.0 \times 10^5 \text{ A.m}^{-1}$ (2.52 KOe), $3.87 \times 10^5 \text{ A.m}^{-1}$ (4.87 KOe) and $7.7 \times 10^5 \text{ A.m}^{-1}$ (9.7 KOe). The calculations were performed with a Texas 59 calculator, producing for each H_a the dependence of M with T . Fig. 9 gives the three curves obtained, plotted in a reduced scale, $M(t)/M(0)$ versus $t = T/T_c$.

We can check whether $\rho_H(T)$ satisfies eq. (53), or its equivalent form:

$$\rho_H / (\mu_0 H_a) = R_0 + R_s (M/H_a) \quad (58)$$

Since R_0 and R_s are practically constant sufficiently above T_c ($T \geq 319 \text{ K}$; see 5.3) we should obtain there a linear plot between $(\rho_H / \mu_0 H_a)$ and (M/H_a) , the corresponding slope and intercept giving R_s and R_0 respectively. Moreover, we should obtain the same straight line irrespective of the particular H_a value used in each experimental run. As shown in Fig. 10, these features are indeed present in our results for the paramagnetic phase. At lower temperatures, considerable deviations from the linear behaviour do appear, more and more important as $T \rightarrow T_c$, and also when H_a is smaller. This is certainly due to the increasing role played by the critical fluctuations, which are not appropriately accounted for with the assumption $R_0, R_s = \text{constant}$ (see 5.3). From the linear plot of Fig. 10 we obtain for R_s :

$$R_s = -2.38 \times 10^{-8} \text{ } \Omega \cdot \text{m} \cdot \text{T}^{-1}$$

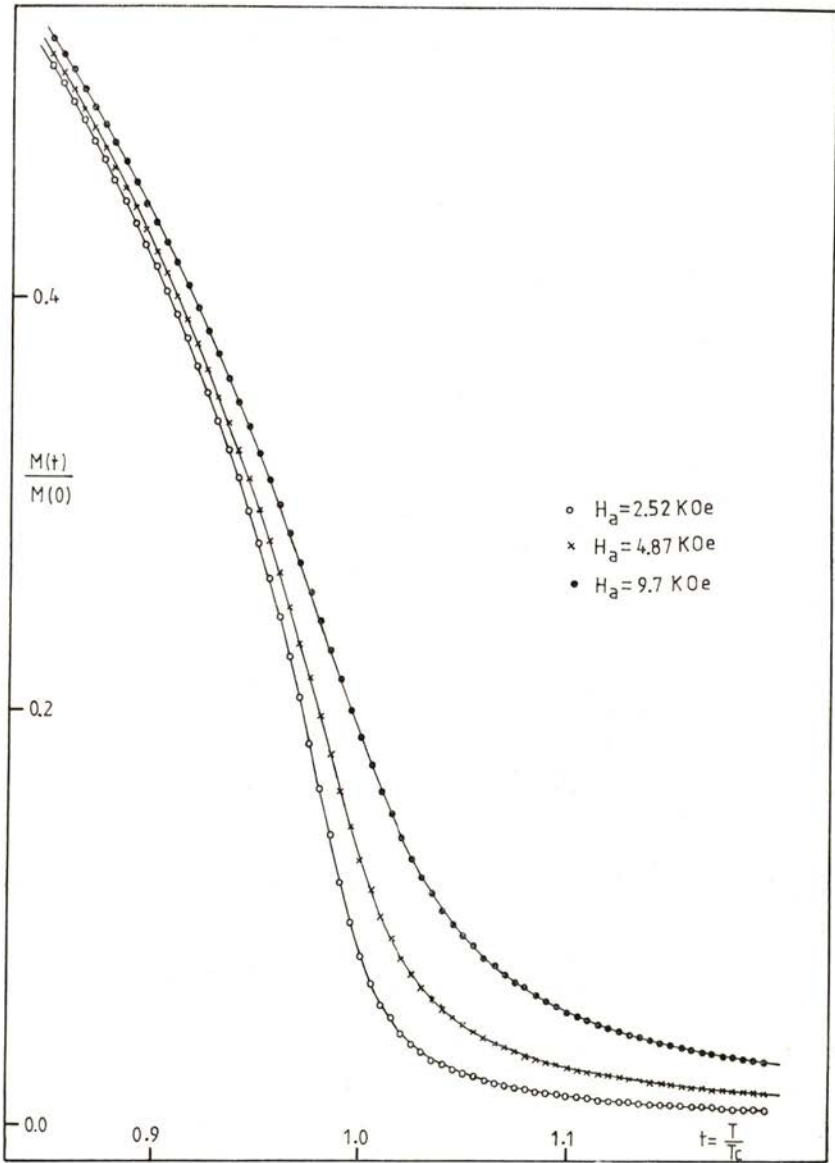


Fig. 9 — Reduced magnetization $M(t)/M(0)$ as a function of reduced temperature $t = T/T_c$; for $H_a = 9.7$ KOe (•), 4.87 KOe (x) and 2.52 KOe (o), calculated from eq. (54) with $D = 1$.

This value is fairly close to the R_s value obtained by Volkenshtein *et al* [30] in a Gd single crystal, $R_s = -2.57 \times 10^{-8} \Omega.m.T^{-1}$. Both values differ considerably from the value previously quoted by

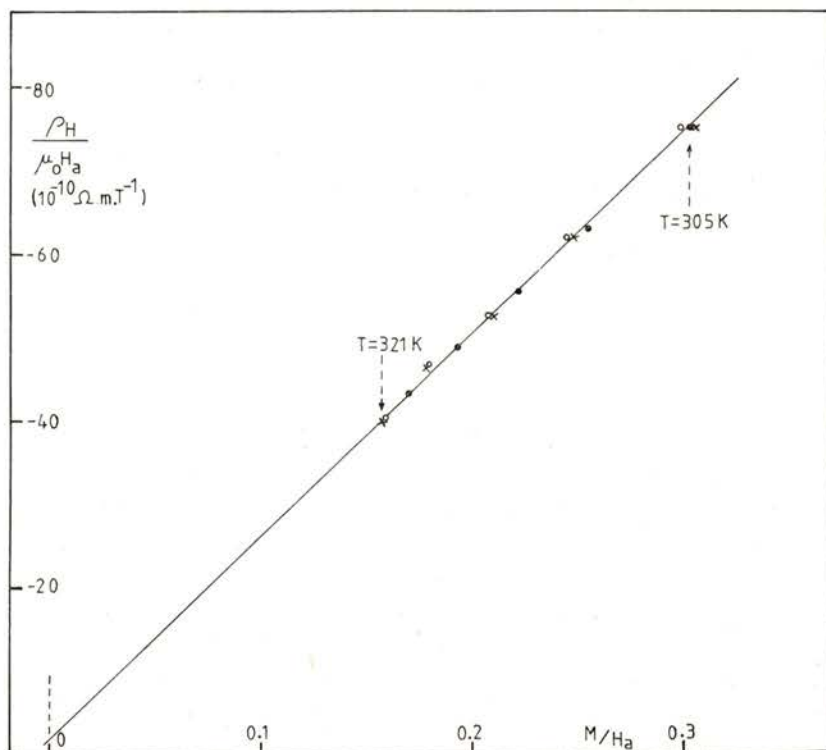


Fig. 10 — In the paramagnetic phase at temperatures sufficiently above T_c , a linear relation occurs between $\rho_H/\mu_0 H_a$ and M/H_a (see eq. 58).

Rhyné [37], $R_s = -1.22 \times 10^{-8} \Omega.m.T^{-1}$. We notice however that in a later work this author and Cullen [18] obtained R_s values of the order of $-2 \times 10^{-8} \Omega.m.T^{-1}$ (at $T \lesssim T_c$), which are considerably closer to our results than his previous value. From the intercept of the straight line in Fig. 10 we obtain:

$$R_0 = -1.92 \times 10^{-10} \Omega.m.T^{-1}$$

This value is considerably higher than the values obtained by Rhyne and Cullen [18] at temperatures near T_c ($-R_0 \geq 0.65 \times 10^{-10} \Omega \cdot m \cdot T^{-1}$) and the values quoted by Vedernikov *et al* [29] from a study of the Hall effect at fairly high temperatures (410 K-800 K; $R_0 = -1.2 \times 10^{-10} \Omega \cdot m \cdot T^{-1}$). We must, however, recognize that the limited range of temperatures available in our case above T_c for the extraction of R_0 from extrapolation of a straight line (319 K-335 K) precludes high accuracy in the corresponding numerical determination.

The calculations of $M(T)/M(0)$ have been repeated with $D = 0.9$ instead of $D = 1$. Only minor changes occur in the results, the new R_0 and R_s values differing by less than 5% from the values quoted above.

5.3 — *Critical region*

We have seen that the temperature dependence of the spontaneous magnetization explains the rapid decrease of ρ_H as T approaches the Curie point. A convenient location of T_c can be obtained from the sharp minimum in the $d\rho_H/dT$ curve. We obtain $T_c = 293 \pm 0.5$ K, in fair agreement with representative data for Gd [23], [24]. Of course, due to the field penetration in the critical region (both above and below T_c), different $1/\rho_H(T_c) \cdot d\rho_H/dT$ curves are obtained with different applied fields H_a , as shown in Fig. 11. However, the minimum in $d\rho_H/dT$ takes place approximately at the same temperature T_c .

Since the magnetic energy of a spin under the applied external fields used in this work is always much smaller than kT_c the shifts in T_c produced by H_a should be fairly small, and so the singularity in $d\rho_H/dT$ indeed occurs at approximately the same temperature.

For the first time, we believe, an attempt is made here to display directly the critical behaviour of the temperature derivative dR_s/dT . For this purpose we took the log-derivative of both members of the relation $\rho_H \approx R_s(T)M(T)$, so as to obtain:

$$\frac{1}{R_s} \frac{dR_s}{dT} = \frac{1}{\rho_H} \frac{d\rho_H}{dT} - \frac{1}{M} \frac{dM}{dT} \quad (59)$$

This relation enables us to extract $(1/R_s) (dR_s/dT)$ directly from the difference between the measured quantity $(1/\rho_H) (d\rho_H/dT)$

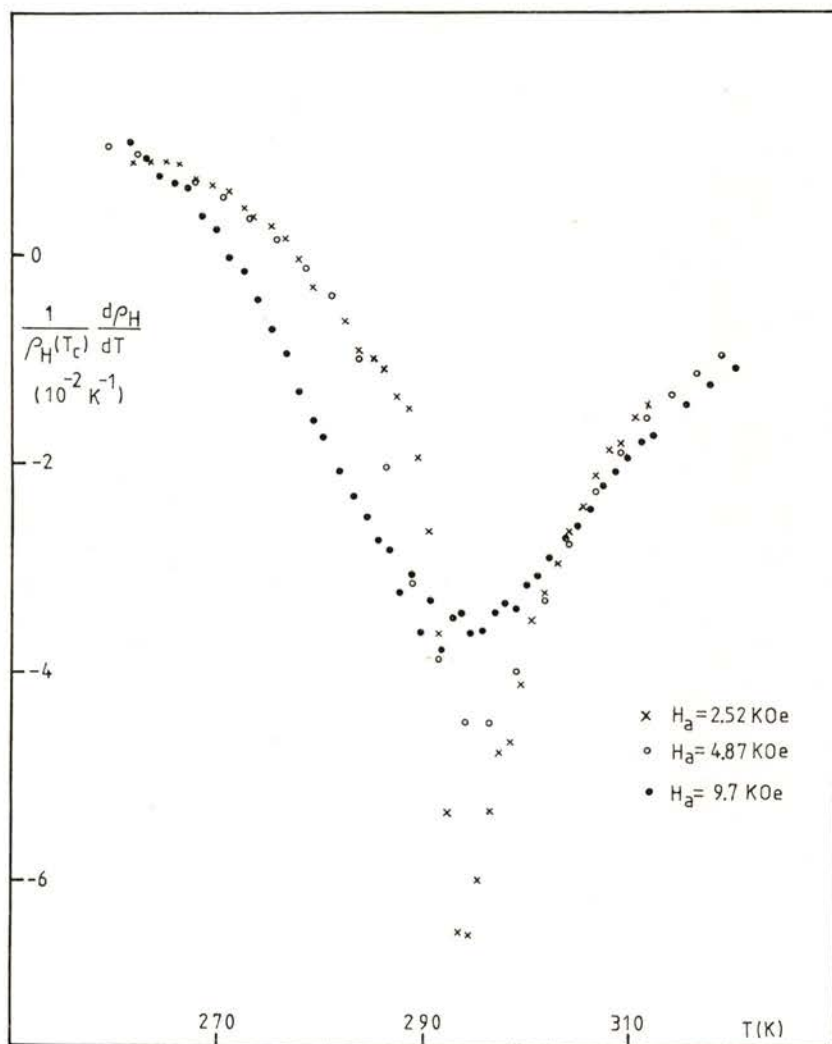


Fig. 11 — Normalized temperature derivative of the Hall resistivity as a function of T , for $H_a = 2.52$ (x), 4.87 (o) and 9.7 KOe (•).

and the calculated magnetization term (from $M(T, H_a)$ given in Fig. 9.). The quantities $(1/\rho_H) (d\rho_H/dT)$ and $(1/M) (dM/dT)$

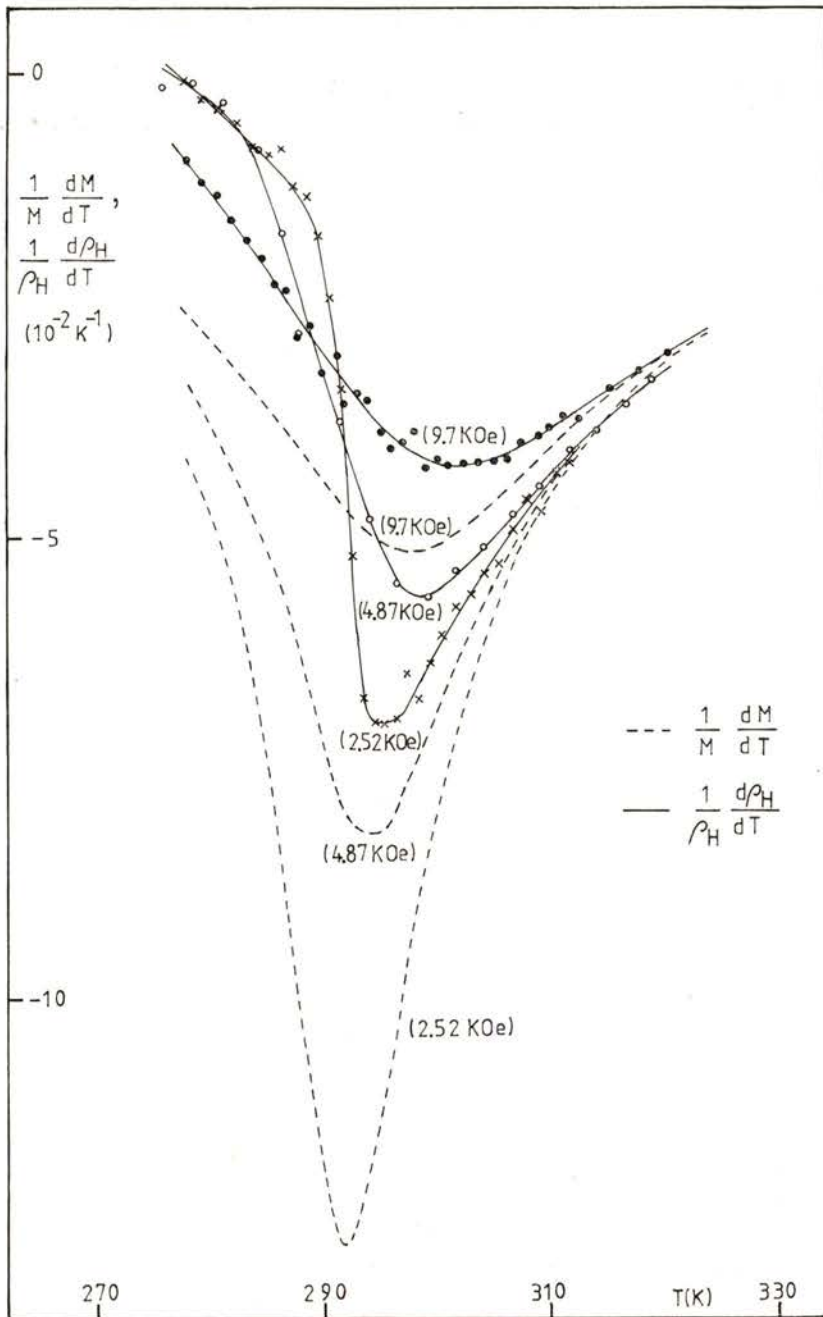


Fig. 12—Temperature dependence of the normalized derivatives $(1/M) (dM/dT)$ and $(1/\rho_H) (d\rho_H/dT)$ near the Curie point of Gadolinium.

for $H_a = 2.52, 4.87$ and 9.7 KOe are displayed in Fig. 12, from which the corresponding coefficients $(1/R_s) (dR_s/dT)$ can be extracted. As shown in Fig. 13, dR_s/dT vanishes at sufficiently

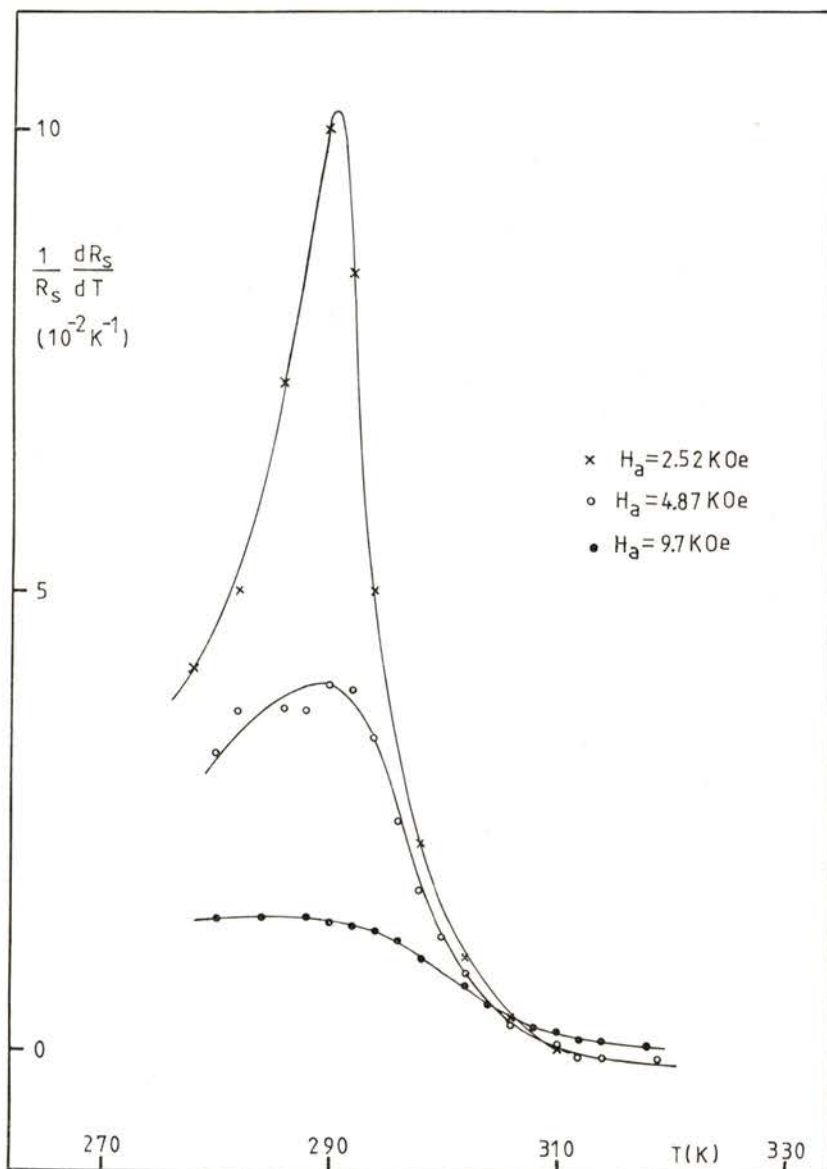


Fig. 13 — Critical behaviour exhibited by the normalized temperature derivative of the extraordinary Hall coefficient R_s , at constant applied field.

high temperatures, where R_s becomes constant. However, as we approach T_c there is a steady increase in R_s , due to the effect of critical fluctuations. This is clearly shown by the curve for the lower field, where dR_s/dT exhibits a sharp peak near T_c , in a manner characteristic of a critical phenomenon [38].

Our results also show an evident slowing down in the «critical features» of dR_s/dT as H_a increases. This is due to the gradual suppression of the spin fluctuations by the applied magnetic field.

Encouraged by these promising preliminary results on the observation of critical features in the temperature derivative of the extraordinary Hall coefficient of Gd, further work is now in progress to investigate ρ_H at lower fields, and to improve, in a first stage, the calculation of the dM/dT derivatives in the paramagnetic phase. At a later stage we aim at the direct measurement of the derivative dM/dT , simultaneously with the ρ_H measurements. Another pertinent question for the future work is the following: which parameter (ρ_H or R_s) is intrinsically more relevant to study the critical behaviour of the Hall effect?

This work has been partially performed under the NATO Res. Gr. 1481, through which the sample of Gd was obtained; in this respect the authors wish to express their gratitude to Dr. D. Hukin and Dr. G. Garton for the sample preparation. Thanks are also due to I.N.I.C. for the financial support provided to perform the work presented here.

REFERENCES

- [1] S. ALEXANDER, J. S. HELMAN, I. BALBERG, *Phys. Rev.*, **B13**, 304 (1976).
- [2] T. G. RICHARD, D. J. W. GELDART, *Phys. Rev.*, **B15**, 1502 (1977).
- [3] T. KASUYA, *Progr. Theor. Phys.*, **22**, 227 (1959).
- [4] S. H. TANG, T. A. KITCHENS, F. J. CADIEU, P. P. CRAIG, *Proc. Conf. Low Temp. Phys.*, **LT13**, Boulder; Plenum, N. Y., p. 385 (1972).
- [5] J. B. SOUSA, R. P. PINTO, M. M. AMADO, J. M. MOREIRA, M. E. BRAGA, M. AUSLOOS, I. BALBERG, *Solid State Communic.*, **31**, 209 (1979).
- [6] Y. SUEZAKI, H. MORI, *Progr. Theor. Phys.*, **41**, 1177 (1969).
- [7] K. KAWASAKI, *Progr. Theor. Phys.*, **29**, 801 (1963).

- [8] K. V. RAO, S. ARAJS, D. ABUKAY, in *Thermal Conductivity* 14, ed. P. G. Klemens and T. K. Chu, Plenum Press, p. 57 (1976).
- [9] I. BALBERG, *Physica*, **91B**, 71 (1977).
- [10] I. BALBERG, J. S. HELMAN, *Phys. Rev.*, **B18**, 303 (1978).
- [11] I. A. CAMPBELL, *J. Mag. and Mag. Mat.*, **12**, 31 (1979).
- [12] See, e. g., *The Hall effect and its Applications*, ed. C. L. Chien and C. R. Westgate, Plenum Press, N. Y. (1980).
- [13] J. P. JAN, in *Solid State Physics*, ed. F. Seitz, D. Turnbull; Academic Press, N. Y., vol. 5, p. 17 (1957).
- [14] L. LANDAU, E. LIFSHITZ, *Electrodynamique des Milieux Continus*, ed. Mir, Moscou, p. 132 (1969).
- [15] J. SMIT, *Physica*, **24**, 39 (1958); J. KONDO, *Progr. Theor. Phys.*, **25**, 722 (1962); A. FRIEDERICH, A. FERT, *Phys. Rev.*, **B9**, 1214 (1974).
- [16] L. BERGER, *Phys. Rev.*, **B2**, 4559 (1970).
- [17] F. E. MARANZANA, *Phys. Rev.*, **160**, 421 (1967).
- [18] J. J. RHYNE, J. R. CULLEN, *Journal de Physique* (Paris) Coll., **C1**, Tome 32, 246 (1971).
- [19] J. B. SOUSA, C. L. SERPA ROSA, P. A. OLIVEIRA LOPES, A. J. RODRIGUES PINTO, *Anais da Faculdade de Ciências do Porto* (in press).
- [20] J. P. JAN, *Helvetica Physica Acta*, **25**, 677 (1952).
- [21] A. BEER; in *Solid State Physics*, ed. F. Seitz, D. Turnbull, Academic Press, N. Y., suppl. 4, p. 50 (1963).
- [22] C. M. HURD, *Hall Effect in Metals and Alloys*, Plenum Press, N. Y., ch. 6 (1972).
- [23] S. LEGVOLD; in *Magnetic Properties of Rare Earth Metals*, ed. R. J. Elliott, Plenum, N. Y., p. 346 (1972).
- [24] S. R. LEE, S. LEGVOLD, *Phys. Rev.*, **162**, 431 (1967).
- [25] M. B. SALAMON, D. S. SIMONS, *Phys. Rev.*, **B7**, 229 (1973).
- [26] J. B. SOUSA, M. M. AMADO, R. P. PINTO, M. F. PINHEIRO, J. M. MOREIRA, M. E. BRAGA, M. AUSLOOS, P. CLIPPE, D. HUKIN, G. GARTON, P. WALKER; in *Recent Advances in Condensed Matter Physics*, ed. J. T. Devreese, L. F. Lemmens, V. E. Van Doren, J. Van Rayen, Plenum, N. Y., vol. 4, p. 115 (1981).
- [27] H. E. NIGH, S. LEGVOLD, F. H. SPEDDING, *Phys. Rev.*, **132**, 1092 (1963).
- [28] B. COQBLIN; in *The Electronic Structure of Rare Earth Metals and Alloys*, The Magnetic Heavy Rare Earths, Academic Press, ch. 9 (1978).
- [29] M. V. VEDERNIKOV, V. G. DVUNITKIN, N. I. MOREVA, *Journal de Physique* (Paris), Coll. **C5**, tome 40, 46 (1979).
- [30] N. V. VOLKENShteIN, I. K. GRIGOROVA, G. V. FEDOROV, *Soviet Physics JETP*, **23**, 1003 (1966).
- [31] N. A. BABUSHKINA, *Soviet Physics-Solid State*, **7**, 2450 (1966).

- [32] F. MARANZANA, *Phys. Rev.*, **160**, 421 (1967); see also J. KONDO, *Progr. Theor. Phys.*, **27**, 772 (1962), B. GIOVANNINI, *Phys. Lett.*, **36A**, 381 (1971).
- [33] YU. P. IRKHIN, SH. SH. ABEL'SKII, *Soviet Physics-Solid State*, **6**, 1283 (1964).
- [34] L. BERGER, G. BERGMAN; in *The Hall Effect and its Applications*, ed. C. L. Chien and C. R. Westgate, Plenum, N. Y., p. 55 (1980).
- [35] A. FERT, *Journal de Physique Lettres* (Paris), **35**, L107 (1974); see also ref. 28.
- [36] D. H. MARTIN; in *Magnetism*, Iliffe Books (1967).
- [37] J. J. RHYNE, *Coll. Int. CNRS n.° 180*, Grenoble, p. 521 (1969).
- [38] H. E. STANLEY, *Introduction to Phase Transitions and Critical Phenomena*, Clarendon Press, Oxford (1971).
- [39] Added in proof: R. ASOMOZA, A. FERT, R. REICH (in press) have developed a theory (based on the predominance of the side-jump mechanism) which accounts for the experimental value of R_s in Gd.